Oceanologia (2020) 62, 511—524

Available online at www.sciencedirect.com

ScienceDirect

journal homepage: www.journals.elsevier.com/oceanologia

ORIGINAL RESEARCH ARTICLE

Combined impact of summer heat waves and coastal upwelling in the Baltic Sea

Ülo Suursaar*

University of Tartu, Estonian Marine Institute, Tallinn, Estonia

Received 22 May 2020; accepted 10 August 2020
Available online 21 August 2020

KEYWORDS
Global warming;
Water temperature;
Salinity;
Marine heat waves;
Satellite images;
Breeze

Summary Under warming climates, heat waves (HWs) have occurred in increasing intensity in Europe. Also, public interest towards HWs has considerably increased over the last decades. The paper discusses the manifestations of the summer 2014 HW and simultaneously occurring coastal upwelling (CU) events in the Gulf of Finland. Caused by an anticyclonic weather pattern and persisting easterly winds, CUs evolved along the southern coast of the Gulf in four episodes from June to August. Based on data from coastal weather stations, 115 days-long measurements with a Recording Doppler Current Profiler (RDCP) oceanographic complex and sea surface temperature (SST) satellite images, the partly opposing impacts of these events are analysed. Occurring on the background of a marine HW (up to 26°C), the CU-forced SST variations reached about 20 degrees. At the 10 m deep RDCP mooring location, a drop from 21.5 to 2.9°C occurred within 60 hours. Salinity varied between 3.6 and 6.2 and an alongshore coastal jet was observed; the statistically preferred westerly current frequently flowed against the wind. Locally, the cooling effect of the CUs occasionally mitigated the overheating effects by the HWs both in the sea and on the marine-land boundary. However, in the elongated channel-like Gulf of Finland, upwelling at one coast is usually paired with downwelling at the opposite coast, and simultaneously or subsequently occurring HWs and CUs effectively

* Corresponding author at: University of Tartu, Estonian Marine Institute, Mäealuse 14, 12618 Tallinn, Estonia.
E-mail addresses: ulo.suursaar@ut.ee, ys@sea.ee
Peer review under the responsibility of the Institute of Oceanology of the Polish Academy of Sciences.

Production and hosting by Elsevier

https://doi.org/10.1016/j.oceano.2020.08.003

contribute to heat transfer from the atmosphere to the water mass. Rising extremes of HWs and rapid variations by CUs may put the ecosystems under increasing stress.

1. Introduction

In the Earth system, contemporary climate change primarily manifests as 'global warming', which nevertheless is a spatially varying and complex phenomenon (IPCC, 2014). Other important interrelated effects are spatio-temporal changes in atmospheric circulation patterns and in wind characteristics, occurring from global to local scales (e.g. Easterling et al., 2000). All these forcings mingle and act on the marine environment causing changes in thermic conditions, hydrodynamics, and ultimately via various links, in biota (e.g. Hoegh-Guldberg and Bruno, 2010; Kotta et al., 2018).

This study addresses the combined effects of atmospheric heat waves and coastal wind-driven upwelling. The study focusses on the year 2014, when in the region of the Baltic Sea, a major summer heat wave (HW) was registered, and in addition, intense coastal upwelling (CU) with a cooling effect along certain, extensive coastline stretches occurred as well.

Based on reports from several scientific agencies around the world, the World Meteorological Organization (WMO) declared 2014 the hottest year on record, then. Globally, the average atmospheric air temperature (AT) was 0.68°C above the 1951–1980 baseline average, which, in turn, was about 0.3–0.4°C higher than the 1880–1920 average (Lenssen et al., 2019). In fact, the record-setting temperature anomalies have continued after 2014. Currently, according to the datasets by the NOAA and NASA, the year 2016 is considered the hottest on record, followed by 2019 and 2015 (Cole and Jacobs, 2020). Due to larger inertia in the oceanic system, the six highest global ocean heat contents have occurred in: 2019, 2018, 2017, 2015, 2016, and 2014 (Cheng et al., 2020). However, Central Europe and the Baltic Sea region has warmed in an even relatively faster pace. For instance, in recent years, the positive anomalies in the Baltic region ATs have been higher by 0.5–1.0°C than the global average (Rutgersson et al., 2015). The total warming trend in the whole Baltic Sea water mass has been 1.07°C for 35 years (1982–2016), while in the upper layer (in sea surface temperature, SST), the increase has been 1.75°C or 0.05°C/year (Liblik and Lips, 2019). While the main AT rise in the Baltic Sea region has occurred in late winter and spring, the SST increase has been faster in summer months (Liblik and Lips, 2019). This can partially be related to the increased frequency and magnitudes of summer HWs, which in turn, cause an increase in marine heat waves (MHWs) (Hobday et al., 2018; Oliver et al., 2019).

Over time, many different HW definitions have been proposed, which vary regarding the target area or study purpose (e.g. Perkins and Alexander, 2013). A HW is usually understood as a period of excessively hot weather lasting from several days to weeks and is measured relative to the weather norms in the area and for the season. Currently, the WMO defines a heat wave as 5 or more consecutive days of prolonged heat in which the daily maximum temperature is higher than the average maximum temperature by 5°C or more (Rafferty, 2020), which concurs with one of the earliest definitions proposed by Frich et al. (2002). However, some nations have come up with their own, slightly different threshold and duration criteria and more definitions and indices describing different aspects of the HW exist in scientific literature (e.g. Keevallik and Vint, 2015; Russo et al., 2014). There is no clear definition of HWs established in Estonia. For instance, while HWs are sometimes considered as periods with daily maxima over 25°C, a gradation of dangerous events includes the ones when the daily maximum exceeds 30°C in two, three, or five consecutive days (EWS, 2020; Õispuu, 2019).

Under warming climates, HWs have occurred in increasing frequencies and magnitudes in Europe (Russo et al., 2015; Schär et al., 2004). The spread and locations of HWs vary greatly. Quite naturally, the most dangerous events are those occurring in densely populated urban areas and in low latitudes. In that sense, the deadliest ones (more than ten thousand casualties per event) probably occurred in France (in 2003) and in Moscow (2010) (Smid et al., 2019). Lying in relative high latitudes, the less populous Baltic Sea region usually suffers from far less HW casualties. Nevertheless, such kind of extreme events may still pose unexpected adverse societal, economic and environmental consequences on high latitudes as well. For instance, exceptionally large cyanobacteria blooms, poisoning water both for human and animal use, have been reported in years with summer HWs in the Baltic Sea (e.g. Kononen and Nõmmann, 1992), and possible further increase in such record-breaking algal blooms have been projected by Meier et al. (2019). Effect of HWs (and MHWs) on the Baltic Sea environment have been studied e.g. by Paalme et al. (2020) and by Takolander et al. (2017). Sea surface warming trends and impacts of HW events in a wider scale have been demonstrated e.g. by Panch et al. (2013), Shaltout (2019), and Wernberg et al. (2013).

Coastal upwelling studies in the Baltic Sea form a much larger pool, including scores of scientific articles (e.g. Delpeche-Ellmann et al., 2017; Gidhagen, 1987; Kowalewski and Ostrowski, 2005; Lehmann et al., 2012; Lips et al., 2009; Myrberg and Andrejev, 2003; Uiboupin and Laanemets, 2009). The CUs in the Baltic Sea can occur site-specifically under suitable meteorological conditions, and in principle, in whatever season. For instance, 'warm' CUs exist in winter (e.g. Kowalewska-Kalkowska and Kowalewski, 2019; Suursaar, 2010). However, summer CUs are still more typical and possibly more influential with much stronger SST imprint. In case of summer CU, persistent alongshore winds (coastline on its left) bring dense,

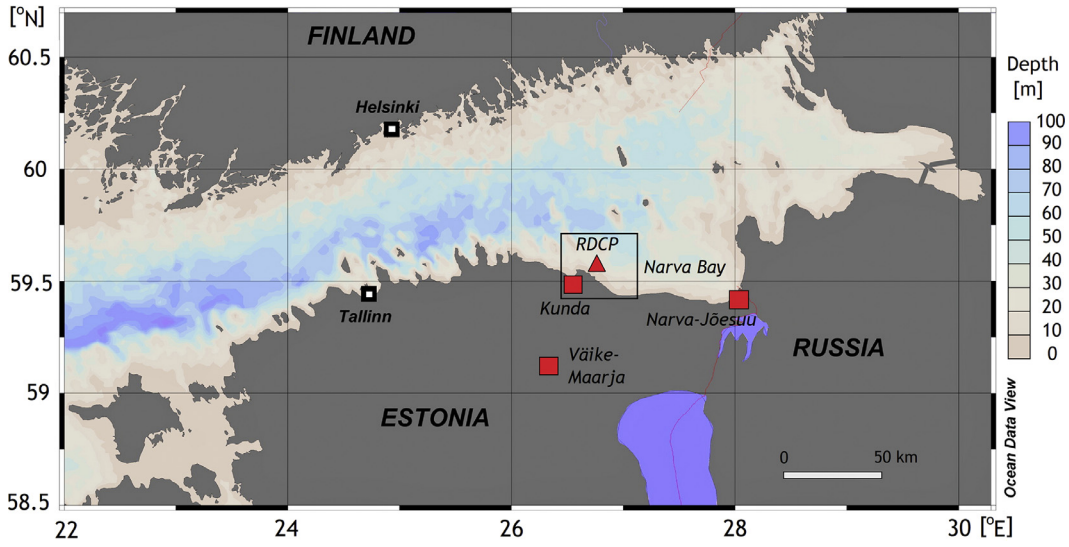

Figure 1 Bathymetric map of the Gulf of Finland (Schlitzer, 2020). Red rectangles mark weather stations by the EWS (Estonian Weather Service), the triangle marks the RDCP (Recording Doppler Current Profiler) mooring location near Letipea Peninsula.

cooler, and usually nutrient-rich water towards the sea surface (e.g. Jiang and Wang, 2018), replacing the warmer and less saline surface water.

Although occurring sometimes simultaneously in certain sea areas, the combined, and possibly opposing effects of HWs and CUs are far less studied so far. Recently, Paalme et al. (2020) studied the effects of HWs and CUs on littoral benthic communities in the Gulf of Finland based on 2018 data. However, under warming climate, study of HWs and their impacts in various conditions and environments is increasingly topical. The aim of this article is to (1) document and analyse the manifestation of the 2014 HW event in the Gulf of Finland (NE Baltic Sea), (2) present and analyse 4 months long in situ oceanographic measurements capturing an extensive CU along the southern coast of the Gulf of Finland in same summer, and (3) discuss the combined effect of simultaneously and/or subsequently occurring HW and CU events on the marine environment and coastal climate.

2. Material and methods

2.1. Study area and the meteorology

The Gulf of Finland is a longitudinally elongated fjord-like sub-basin of the Baltic Sea (Figure 1), located on the relatively high latitudes (59—60.5°N) in the temperate climate zone of prevailing westerlies (Kont et al., 2011). It has an area of 29 571 km^2, water volume of 1103 km^3, and an average depth of 37 m with maximum values reaching 123 m in the westernmost part of the Gulf (Alenius et al., 1998). It receives a relatively large (114 km^3/yr) freshwater input from rivers (mainly via the Neva, Narva, and Kymijoki) and the typical surface salinity varies between 1 and 7 PSU lengthwise and, in the deeper western part, between 6 and 12 units vertically (Alenius et al., 1998).

Our study focuses mainly on the south-eastern part of the Gulf of Finland, where the broad Narva Bay defines a roughly 100 km long, relatively straight coastal section between the Narva River mouth and Kunda-Letipea area on the southern shore (Figure 1). Owing to its elongated shape, upwelling can occur along both coasts. The relatively straight southern coast has a more suitable coastal slope for upwelling evolvement (Delpeche-Ellmann et al., 2018). On the other hand, due to statistically prevailing westerlies (Soomere et al., 2008), the occurrence of upwelling is higher on the northern shore (Lehmann et al., 2012; Myrberg and Andrejev, 2003).

Meteorological description of this study is based on data from the Estonian Weather Service (EWS, 2020; formerly the EMHI). The closest station to our oceanographic instrument mooring location near the Letipea Peninsula is at Kunda (59°31′17″N; 26°32′29″E; 8 km from the RDCP), where we used hourly average wind speed and direction data, as well as air temperature and water temperature data (measured at nearby Kunda Port). The wind data were used to analyse upwelling-favouring forcing conditions, AT data for defining HW periods, and water temperature data for describing effects of HWs and MHWs on the marine environment. From Narva-Jõesuu (59°28′06″N; 28°02′33″E; 77 km from the RDCP) we only used water temperature data. From Väike-Maarja station, (59°08′29″N; 26°13′51″E), 45 km inland from Kunda Port (Figure 1), we used air temperature data to analyse the temperature differences between the coast and an inland location. Since 2003, all the stations are equipped with MILOS-520 automated weather complexes (see: Keevallik et al., 2007).

In order to consider climatic background conditions in Estonia, we also used various web-based annual overviews by the EWS (e.g. Kallis et al., 2015), as well as its statistics on climate normals (EWS, 2020).

2.2. In situ oceanographic measurements

Studies on hydrodynamic conditions near the Letipea Peninsula and in the Narva Bay have been carried out several times since 2006. It turned out that along the straight coastline section, illustrious upwelling events can be occasionally recorded and analysed (Suursaar and Aps, 2007). Using

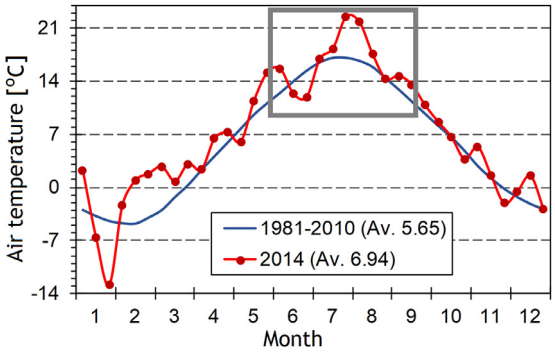

Figure 2 Variations in air temperature at Kunda weather station (10-day averages in 2014) compared with 1981–2010 long-term average (EWS data). The window defines the 4-months study period in summer 2014.

bottom-mounted current profilers, CTD-probes and other devices, more than a years' worth of recordings on various hydro-physical and chemical parameters have been obtained in that location over 2006–2010 (Suursaar, 2010, 2013). This article stems from nearly 4-month long measurements at the same location in 2014 (Figure 2), which have never been analysed and published before.

In 2014, the measurements were carried out using the oceanographic measuring complex called Recording Doppler Current profiler (RDCP-600) by AADI Aanderaa (currently YSI, a Xylem brand). The upward-looking instrument was deployed on the seabed (about 2 km off the coast at 59°33′30″N; 26°40′10″E; Figure 1) by divers from a speed boat of the Estonian Marine Institute and it started autonomous recording on 6 June 2014 at 12.00 UTC. The instrument depth was about 10–11 m (it changed a bit along with water level variations) and the recording interval was set to 60 min. The instrument was retrieved on 29 September 10.00 UTC, producing 2758 hourly records (114.9 days).

The recorded parameters were, firstly, three velocity components (u, v, z) on a multitude of depth cells. The vertical column set-up for flow measurements included a 2 m cell size with no overlap. Due to relatively shallow water, we used 3 depth intervals (3–5, 5–7 and 7–9 m). Beginning with the seabed, there was a 2 m blank distance between the instrument and the lowest measurable cell. Within the 1–3 uppermost metres, depending on sea-level variations and wave height, the flow measurements were somewhat "contaminated" and thus discarded on the grounds of high standard deviations.

In addition to Doppler effect-based current measurements, the RDCP-600 was equipped with temperature, oxygen, pressure, turbidity and conductivity (i.e. salinity) sensors, which sampled hourly the near-bottom layer (0.4 m from the seabed) in contact with the instrument (see also Suursaar, 2010). The high accuracy quartz-based pressure sensor (resolution 0.001% of full scale) enabled measurement of wave parameters, such as significant and maximum wave heights (H_s, H_{max}), as well as various derivations of wave periods (not discussed in this article). The raw data were stored on a multimedia card, processed upon retrieval by the special software by AADI, and thereafter, using packages such as Statistica. Cumulated water (and air) flow components (u-, v-) were computed for the Kunda location, temporal variations in observed parameters studied, and regression and spectral analysis performed.

2.3. SST images

In order to describe SST spatial patterns in the Gulf of Finland during HW and CU periods in 2014, satellite images processed in the Finnish Environment Institute (SYKE) were used. Based on raw data from several NASA, NOAA and EU Copernicus program instruments, SYKE Geoinformatics systems and Geoinformatics research units have produced downloadable remote sensing products (e.g. SST, turbidity, CDOM and Chl *a*). For 2014, SST images based on NOAA AVHRR (NOAA) satellite observations (mediated by the Finnish Meteorological Institute) were downloaded from SYKE TARKKA open web service (http://syke.fi/tarkka/en). In principle, the images are available on a nearly daily basis. However, their usefulness varies due to cloudiness.

Over the 4-month period (June–September), 93 images were reviewed and visually assessed. Our preliminary assortment yielded 8 particularly good SST-images for our study area (i.e. the Gulf of Finland and particularly its southern half). Additionally, 7 images were satisfactory (i.e., partially usable), while the remaining 78 were not that usable (Figure 3a). Still, both the HW and CU periods, as well as post-upwelling conditions, can be successfully illustrated by the SST images.

3. Results and discussion

3.1. Year 2014 case: air and water temperature

The summer 2014 HW, also sometimes called the "2014 Swedish heat wave" (Russo et al., 2015), was caused by a large and stable atmospheric high pressure aloft which remained over north-eastern Europe for several weeks, blocking westerlies and cyclonic activity along the polar front in this region. According to synoptic maps by EWS and SMHI, the high-pressure area covered the entire of Scandinavia and the Baltic Sea. It extended up to Svalbard and Novaya Zemlya in the North and down to Belarus and Ukraine in the South-East. Several heat records were broken in Sweden, as well as in Finland and elsewhere. According to the ranking of European record-breaking HWs in the period of 1950–2015 by Russo et al. (2015), the exceptionally long Scandinavian July–August 2014 event went to the top ten list of the 65-year period. The HW in 2014 also caused a MHW in the Baltic Sea and an overall warming of the Baltic Sea water mass. The annual mean SSTs of the entire Baltic Sea was 9°C in 2014, which was the warmest at the time and 1.14°C higher than the average in 1990–2018 (Siegel and Gerth, 2019); this anomaly was only surpassed in 2018 (which was 1.19°C higher).

According to the 2014 yearbook by the EWS (EWS, 2020; Kallis et al., 2015), the summer was unusually warm also in Estonia (Figure 2). In retrospect (1951–2018), the most influential HWs in Estonia have occurred, starting with the most influential, in 2010, 2018, 2014, and 2003 (the order may slightly vary depending on criteria). This list partly reflects the warming trend, including the 2 degrees increase

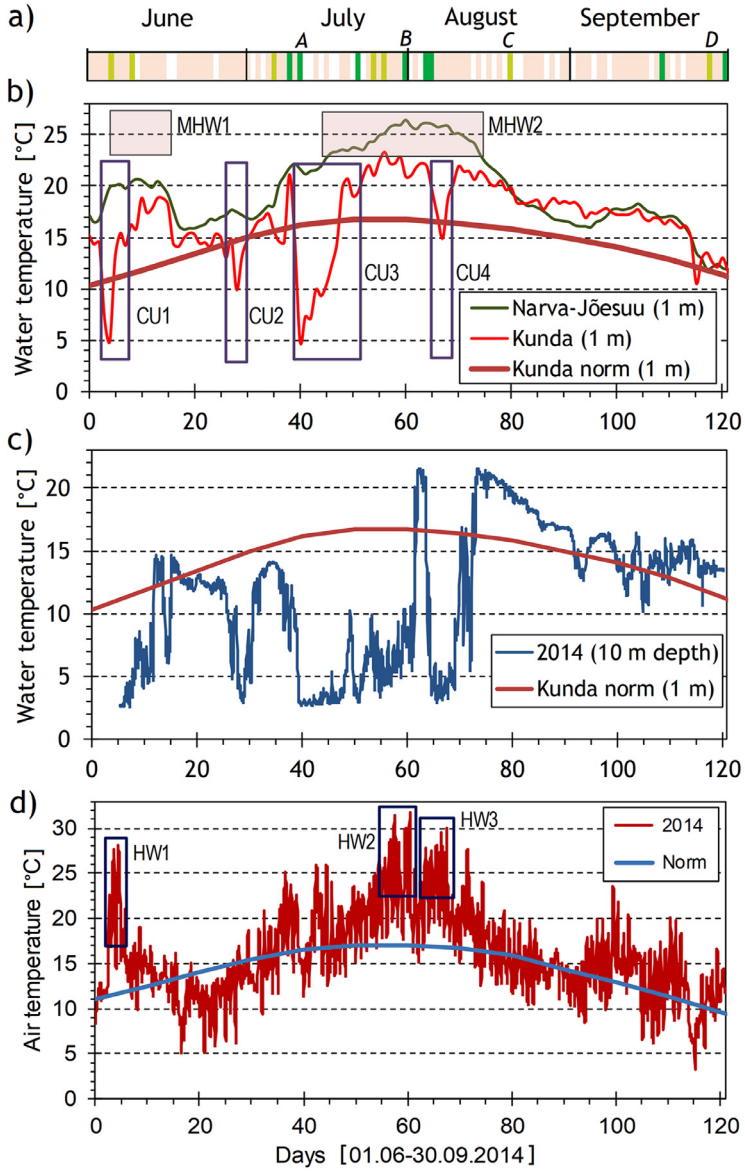

Figure 3 (a) Availability of SST images during the 4-month period; dark green — particularly good image, light green — satisfactory image, pink — limited coverage, white — no image. Letters A—D mark the chosen images on Fig. 4. (b) Water temperatures at Narva-Jõesuu and Kunda weather stations (EWS afternoon data) in 2014, Kunda long-term normal, MHW — marine heat wave events, CU — Kunda station based coastal upwelling events (Table 1). (c) Variations in water temperature measured hourly near Letipea Peninsula at 10 m depth. (d) Air temperatures measured hourly at Kunda weather station compared with long-term normal; HW — heat wave events based on Kunda weather data.

in maximum air temperatures over the same 68-year period (Õispuu, 2019). At Kunda station, July was on average 3°C warmer than the norm (16.3 vs. 19.3°C) and August was 2.4°C warmer (15.4 vs. 17.8°C). As a result, the whole year was 1.3°C warmer than the norm (1.4°C warmer in entire Estonia). Some clear HW events can be identified in the study area (Figure 3).

Considering the simple criteria (daily average exceedance by at least 5 degrees over a long-term normal on at least 5 consecutive days), there were 2 proper heat waves at Kunda location (HW2 and HW3, Figure 3) and one remarkable event which barely did not qualify (HW1). Daily maxima in this coastal town exceeded 30°C in four days. According to the EWS Kunda data, the HW1 event occurred on 4—6 June. It lasted at least 3 consecutive days (actually nearly 4 days), however, the daily average normal was exceeded by about 10 degrees on two consecutive days. HW2 occurred on 25—31 July (7 days) and HW3 on 3—7 August (5 days). The maximum value (32°C) was measured on 31 July. There were some other relatively warm periods around 13 July, 11 August, and 8 September, which were either shorter or not so extreme to be considered as HWs (Figure 3d). However, in other weather stations, the HW periods and durations could have been slightly different.

Following a similar criterion, marine heat waves (MHWs) occurred in Kunda (at port, 1 m depth) on 10—15.06 (MHW1,

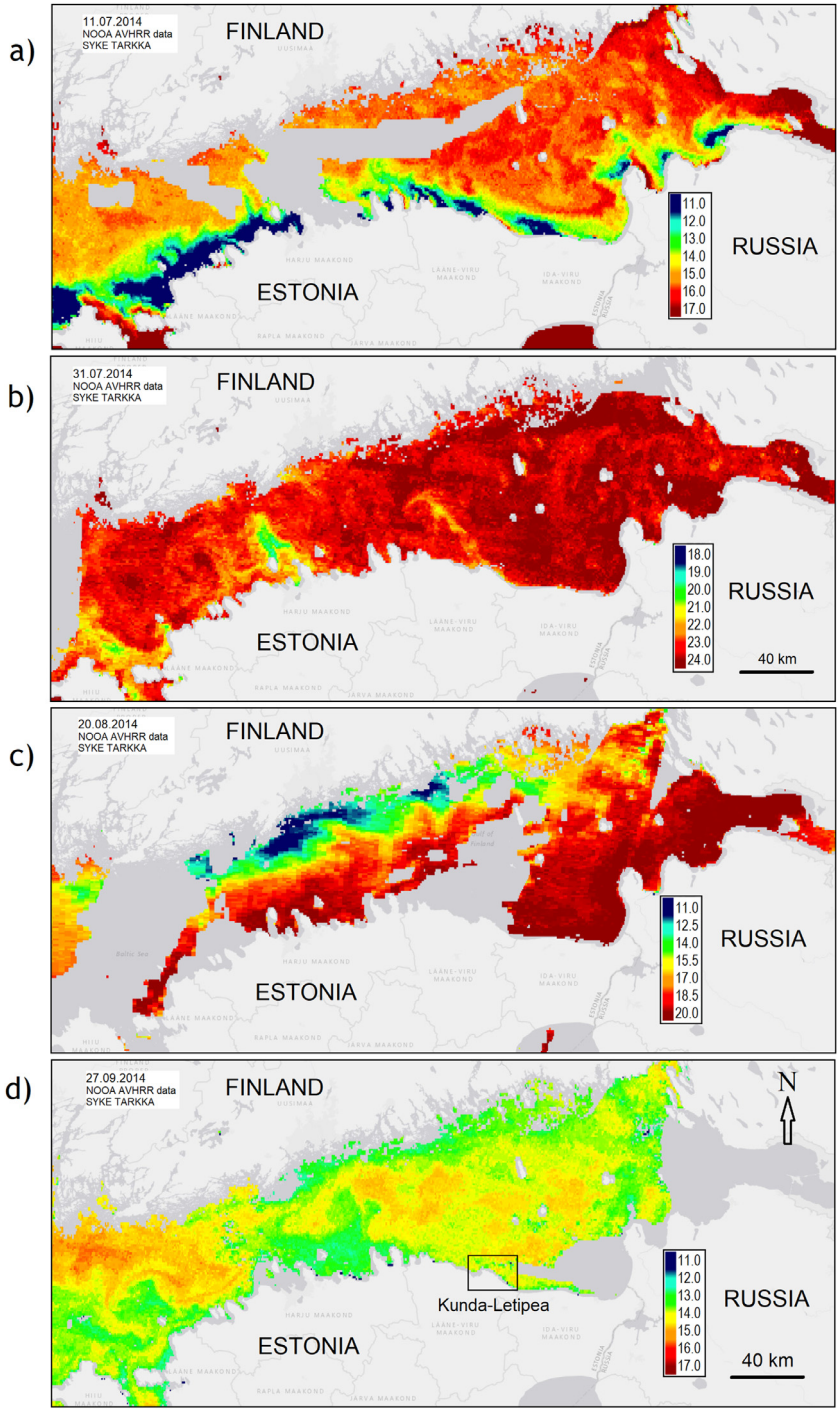

Figure 4 SST images (modified from SYKE TARKKA) during upwelling along the Estonian coast (a, 11.07), MHW (marine heat wave events) covering the entire Gulf (b, 31.07), upwelling at the Finnish coast (c, 20.08), mixing and cooling (d, 27.09).

6 days) and on 24–30.06 (MHW2, 7 days plus 3 more days after a short recession). In Narva-Jõesuu, MHW1 occurred on 4–16.06 (13 days) and MHW2 on 16.07–15.08 (31 consecutive days). MHWs at Kunda were occasionally interrupted by CU events (Figure 3b). In contact with the RDCP at 10 m depth, the summer water temperatures were obviously somewhat smaller and upwelling-influenced water temperature drops were much more extensive than at near-surface (Figure 3c). However, even there, the RDCP yielded remarkably high water temperature anomalies (defined here as exceeding by 5 degrees the 1 m depth normal; 10 m depth normal is unknown) on 2–3 August (up to 21.5°C on 2 August) and on 5 consecutive days on 13–17 August (max 21.5°C on 13 August).

The highest measured water temperature at Kunda port was 23.3°C (on 27 July). At Narva-Jõesuu, it reached 26.5°C

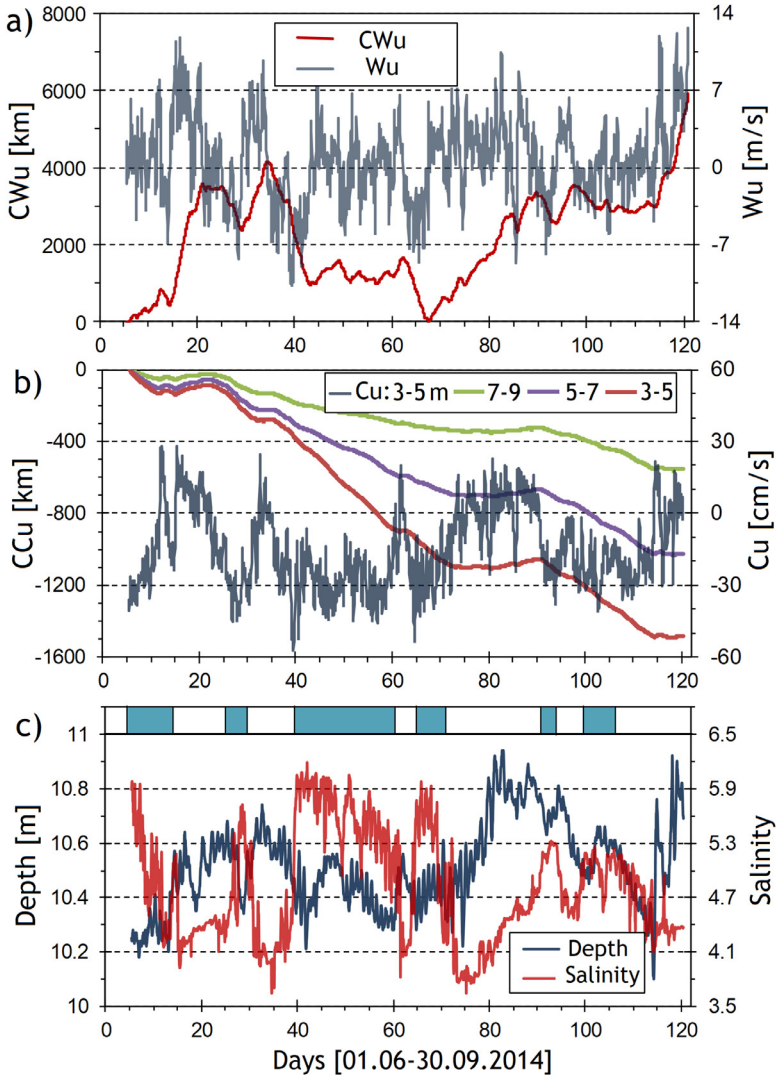

Figure 5 Variations in hourly wind u-component and cumulated u-component at Kunda station (u is nearly shore-parallel at Letipea Peninsula) positive direction of the vector is East; a); RDCP-measured flow u-component at 3—5 m depth and cumulated u-components at 7—9, 5—7, and 3—5 m layers (b); variations in salinity and instrument depth (sea level; c). Blue bar on (c) indicates upwelling impacts, including elevated salinity at 10 m depth and westerly-directed current.

Table 1 CU event durations and minimum water temperatures (WT,°C) at Kunda station (1 m) and RDCP mooring at Letipea Peninsula (10 m); see also Figure 3.

	Kunda	WT	Letipea	WT
CU1	03.06—07.06	4.7	(03.06)—12.06	2.6
CU2	26.06—29.06	8.1	26.06—01.07	2.9
CU3	10.07—17.07	4.9	09.07—01.08	2.7
CU4	05.08—07.08	14.5	04.08—12.08	2.9

on 30 July and stayed at 26.2°C for three consecutive days on 3—5 August (Figure 3b). In contrast, the water temperature at Kunda dropped down to 4.7°C during CU1, 8.1°C in CU2, 4.9°C in CU3, and 14.5°C in CU4 (Table 1), which marks nearly 20°C SST variations.

According to SST images, CU can cover the entirety of Estonia's 360 km-long northern coast from Hiiumaa Island in the West to Narva-Jõesuu in the East and extending for about 100 more km-s along the Russian coast (Figure 4a; Uiboupin and Laanemets, 2009). The cross-shore extent of the affected sea area can be up to 25 km, filaments excluded. While CU occurs on one side of the Gulf of Finland, MHW can occur in rest of the basin (Fig. 4a, c). Under unfavouring wind conditions for CUs on either coast, MHW can cover the entire Gulf. For instance, on 31 July, even the 'coldest' patches had SST around 20°C, while 90% of the Gulf's area had SSTs between 23 and 24 (or more) degrees (Figure 4b). CU duration varies depending on coastal location. The periods CU1-CU4 were identified based on Kunda SST (Figure 3b). However, the upwelling process is visible from RDCP data over a much longer period because it manifests in deeper layers before it reaches the sea surface. It also lasts longer (Figure 3c). Out of 115 measurement days, CU impact was visible on about 50 days at the 10 m depth and on 20—25 days on the sea surface near Kunda (Table 1).

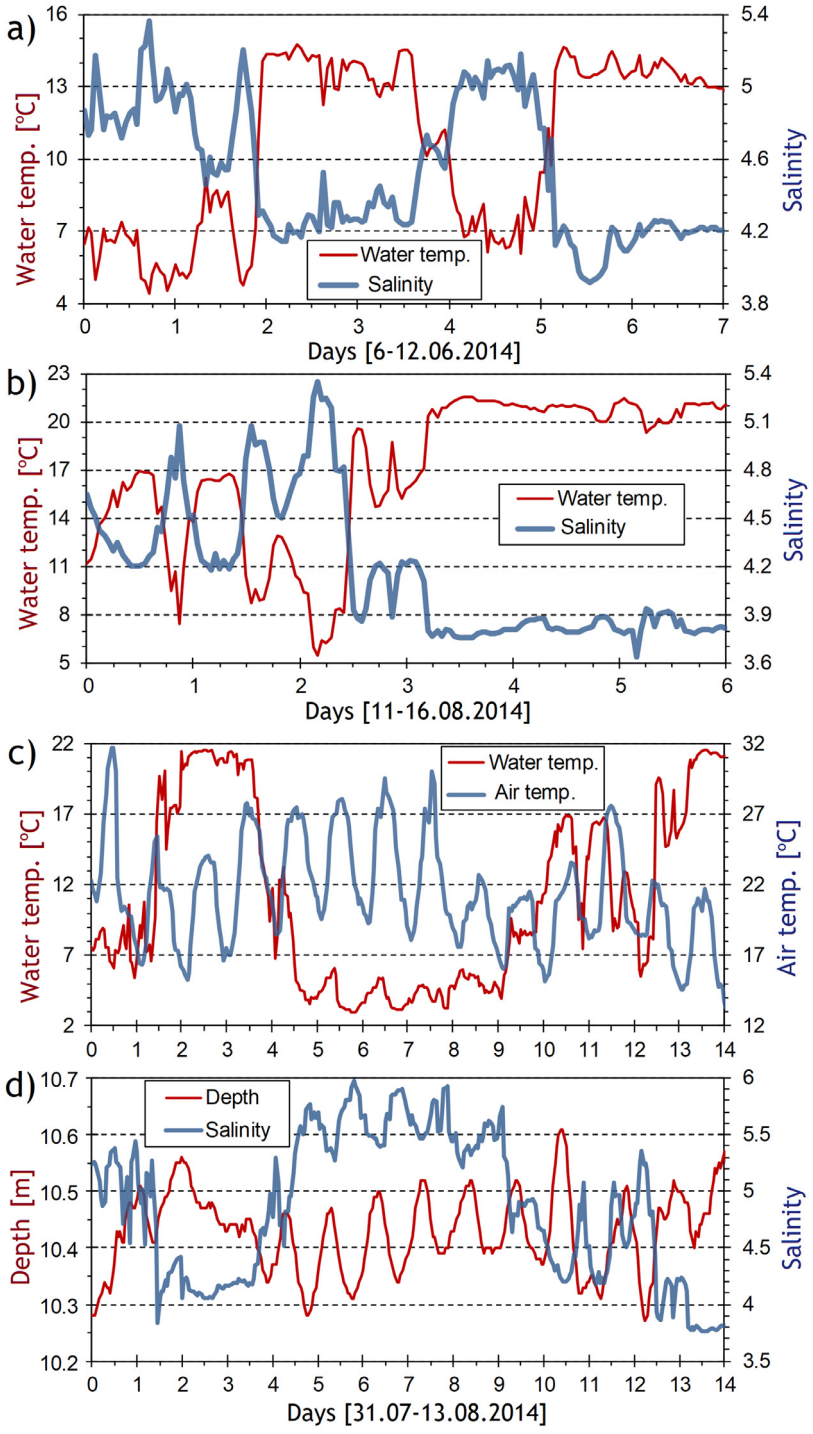

Figure 6 Contrasting variations in water temperature and salinity indicating upwelling at 10 m depth (a, b); Diurnal variations in air temperature at Kunda, also impacting (via daily switching breeze) water temperature (smaller oscillations besides large upwelling-caused variations), salinity and local sea level (c, d).

While the summer of 2014 was among the most extreme ever recorded regarding water temperatures and MHWs (Siegel and Gerth, 2019), CUs are rather common, occurring along the northern coast of Estonia roughly every other year (Uiboupin and Laanemets, 2009). In terms of extent and duration, the summer 2014 CUs probably were not among the largest. For instance, the year 2003 event and the 2006 event (e.g. Suursaar and Aps, 2007) were more extensive. However, in terms of water temperature variation, 2014 was remarkable due to opposing effects of CU and MHW, occurring on the background of very high water temperatures. For instance, at Kunda station, a 17.1°C SST drop occurred within 50 hours. At the RDCP, an 18.6°C drop (from 21.5 to 2.9°C) occurred in two and half days (60 hours), including

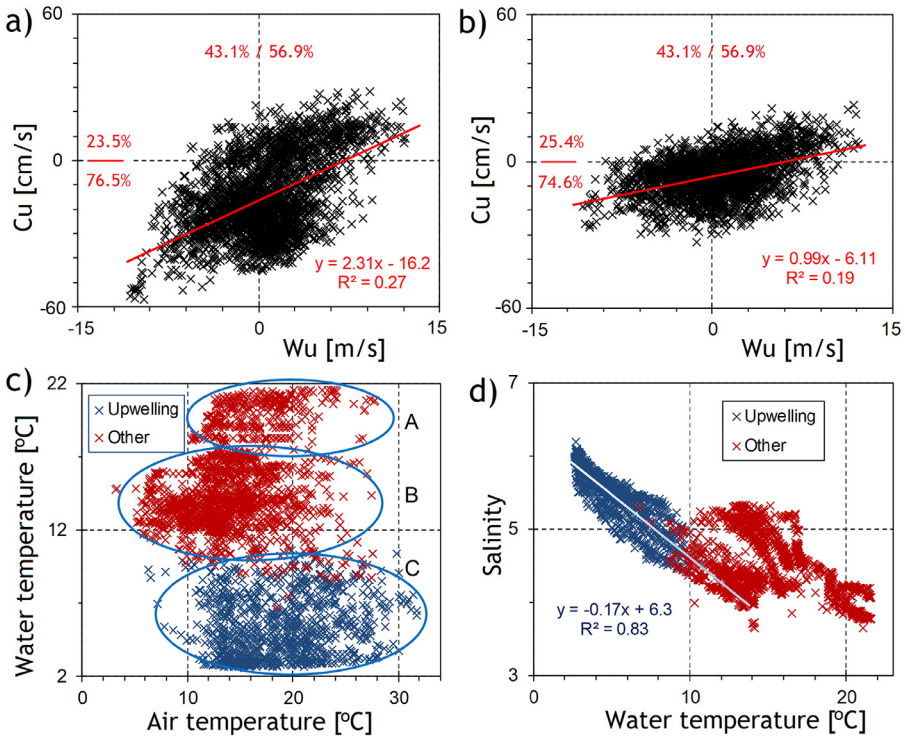

Figure 7 Plots of wind and flow u-component values at two depths (a — sub-surface, b — near-bottom) indicating preferred West-directed current occurring even in moderate West wind conditions. Plots of air versus water temperatures (c) and water temperatures versus salinity (d) indicating differently behaving data subsets under upwelling and non-upwelling conditions. Zone C (on c) marks CU, zone A mostly marks post-upwelling MHW (marine heat wave events) in August, and zone B pre-upwelling periods in June and cooling period in September.

a 24 h drop of 15.7°C. The total range was over 20°C both temporally (Figure 3) and spatially (considering maximum SSTs over 26°C; Figures 3b, 4).

3.2. Upwelling development and its effects on water column properties

It is a well-known fact that mesoscale CU is triggered by the alongshore wind component, causing Coriolis force assisted Ekman transport of surface water away from the shore, which is replaced by water that wells up from below (e.g. Gill and Clarke, 1974). It is also described that favourable alongshore winds should last for at least a few days until certain cumulative wind impulse is reached (e.g. Haapala, 1994) and upwelled water surfaces, thus becoming 'visible'. In fact, bottom-mounted instruments can show near-instantaneous changes in virtually every measured parameter (Figures. 5–6) and CUs are manifested over longer periods than on the surface (Table 1). Based on Figure 5, CU favouring conditions occur on the southern coast of the Gulf of Finland when the alongshore wind component (u-component) is mostly negative (West-directed) and cumulated u-wind decreases (Figure 5a); current u-component is negative and cumulated u- decreases, especially in sub-surface layers (Figure 5b); salinity is relatively high or increasing and water level decreases (Figure 5c).

As a result of up-flow of more saline and cooler intermediate or deep layer water of the Gulf, water temperatures and salinity graphs form distinct negatively correlated patterns (Figure 6ab, 7d). Besides dramatic (up to 20°C) fluctuations in water temperature, salinity varied between 3.6 and 6.2 (Figures 5c, 6), which is rather remarkable for this brackish water location. The correlation coefficient between water temperature and salinity was −0.82 over the entire 115-day period.

A curious feature of the Letipea coastal section is that under statistically prevailing westerly winds both above the Gulf (e.g. at Kalbådagrund; Westerlund et al., 2018) and at Kunda (Suursaar, 2013), just a relatively weak easterly is required to cause a west-directed rapid alongshore current — an upwelling-related coastal jet (Figure 5). Even more, water easily flows against the wind at Letipea (Figure 7ab). Over the 115-day study period in 2014, the wind u-component was positive in 56.9% cases. At the same time, only 23.5% of sub-surface current u-components were accordingly positive (Figure 7). The same feature has been described in previous moorings as well (Suursaar, 2010). The finding also fits with the simulation results with eddy-resolving models (Andrejev et al., 2004; Soomere et al., 2008), showing a topographically modified, quasi-permanent clockwise gyre, yielding a resultant westward current along the coast between Narva-Jõesuu and Kunda. According to modelling study by Westerlund et al. (2019), this 6–10 cm/s resultant flow occurred at Letipea throughout all seasons, being just somewhat weaker only in autumn. Based on our 293 + 115 days of in situ measurements (from previous mooring plus this study), the W current occurred on 73% of cases on the sub-surface layer (resulted u =

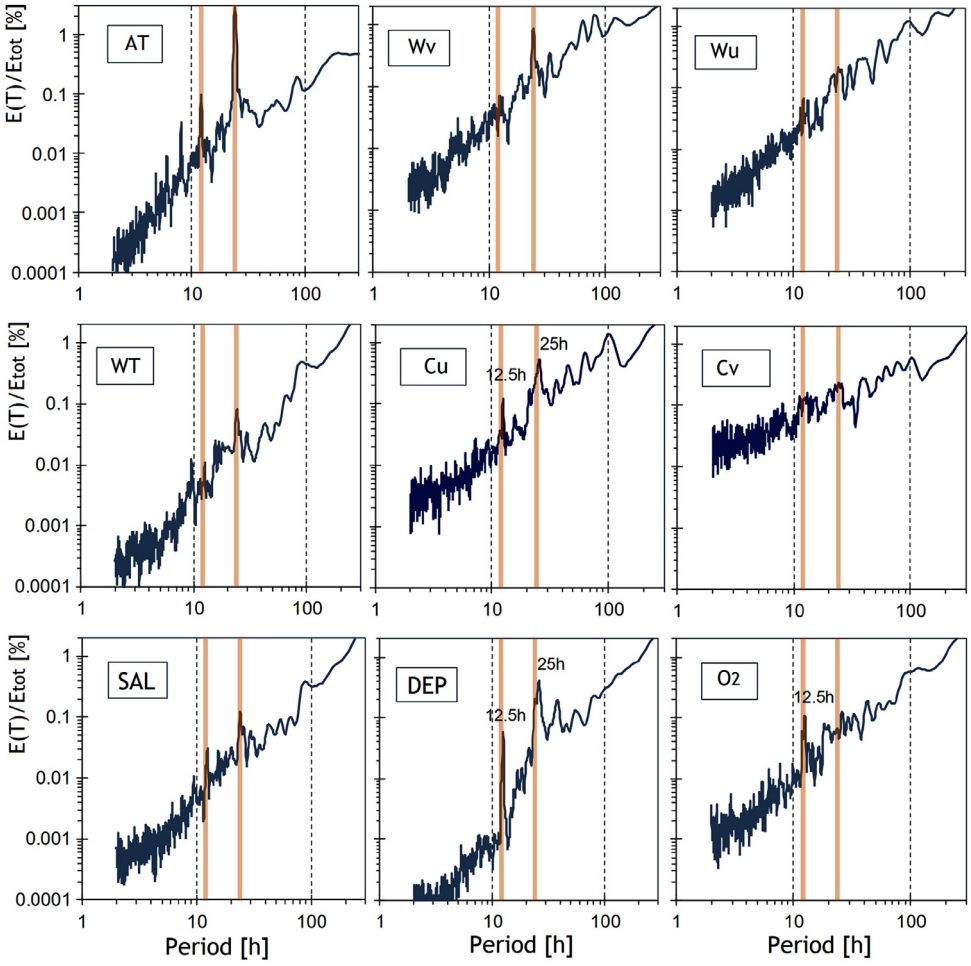

Figure 8 Normalized spectra (total energy =100%) calculated from hourly meteorological data from Kunda station (AT — air temperature, Wv and Wu — wind v- and u- component, respectively) and from hourly RDCP data measured at 10 m depth near Letipea Ps. (WT — water temperature, Cu, Cv — current u- and v-component at the lowermost cell, SAL — salinity, DEP- instrument depth, O2 — water oxygen content). Vertical lines mark diurnal (12, 24 h) periods, 12.5 and 25 h are specifically indicated, when the main peaks occur on these periods instead of strictly diurnal harmonics.

—9 cm/s), while in the near-bottom layer, W and E currents were practically balanced. While E-directed current was vertically rather homogeneous, the W-current, especially during CU, was stratified with higher values in upper layers (up to 61 cm/s at 3—5 m depth and 67 cm/s at the discarded 1—3 m depth range). Low values or even backflows occurred in deeper layers. This also appears on cumulated u-current graphs (Figure 5b), which diverge faster from each other during CU periods. Despite occasional west-storms, we have never registered a faster E current than 46 cm/s at Letipea, while the maximum W current 76 cm/s has been recorded in relatively modest (3—5 m/s, gusts up to 8 m/s) E-wind conditions, clearly indicating an upwelling-related coastal jet (Suursaar, 2010).

3.3. Combined effects of HWs and CUs on local and basin-wide scales

Several simultaneous processes with sometimes opposing effects occur in the sea. Firstly, impacts of HW and CU occasionally mingle on the local scale (Figures 3, 6). Instead of being around 20°C, water temperature may drop against seasonal norms down to 4—5°C in the surface layer and to 3—4°C at the 10—11 m depth. This can happen even in the hottest days when the air temperatures reach 25—32°C. These HW and CU-caused deformations in water temperatures are well visible in Figure 3c. Therefore, the connection between air and water temperatures is not straightforward, especially when CU is involved (Figures 6c, 7c).

In addition to these mesoscale (in temporal scale — days-weeks) processes, clear diurnal variations are visible in air and water temperatures, but also in salinity and depth (Figure 6cd). The main driving force behind these variations is daily variation in air temperature, which, under stable anticyclonic weather and HW conditions may reach 10 degrees or more (e.g. 16 vs. 32°C on 31.07, 19 vs. 30°C on 07.08) even at coastal locations. Such periodic diurnal variations also cause variations in atmospheric pressure and local winds, known as (daily) sea and (nightly) land breeze. Spectra calculated from hourly records with similar 115-days extent (Figure 8) clearly show prominent peaks and its harmonics (24 h, 12 h) in air temperature (AT, see Figure 8 for the following abbreviations). The same periods, though less prominent, also occur on WT. Further on, the 24 h peak at Wv shows the presence of cross-shore winds (breeze), while in Wu the diurnal peak was missing. Wv in turn evokes variations in alongshore current (Cu) and depth. However, these peaks did not occur strictly on diurnal periods but were somewhat modified by inertial and tidal periods, which yielded peaks at 12.5 h and 25 h, instead. Slopes of the spectra and the share of long-period (>100 h) variations (Figure 8) described atmospheric synoptic processes, including the variations due to CU and HW. The share of such motions was relatively large in wind data (Wu, -v), Cu and depth, but also in WT and salinity (due to strong CU-related variations). The gentle slope in Cv is due to the lack of freedom in cross-shore water movements in the nearshore location.

Besides the contrasting impacts on water column properties discussed above, the combined effects of CU and HW may also include some other aspects. Firstly, there is an important impact of CUs and HWs on basin-wide mixing and water column warming. Up- and downwelling are the major agents of mixing in the Gulf of Finland. Average properties of the water masses across the gulf may be substantially modified by sequences of upwellings and downwellings (Delpeche-Ellmann et al., 2017; Soomere et al., 2008; Talpsepp, 2008). In a stratified sea, heat transport from the surface to deeper layers is a slow process (Figure 9a) unless aided by vertical mixing due to surface and internal waves, shear entrainment, turbulence and upwelling (e.g. Elken et al., 2015; Strange and Fernando, 2001). Moreover, in elongated channel-like basins like the Gulf of Finland, upwelling at one coast is usually paired with downwelling at opposite coast (Figure 9b). Obviously, heat transport during HW is faster and more effective in such up/downwelling conditions rather than without it — in calm anticyclonic conditions or under non-persistent wind conditions (Figure 9).

Delayed heat transfer from the surface into deep layers is confirmed by the fact that, over the last decades, water temperature in the upper layer has increased faster in the Baltic Sea than the whole water mass (Liblik and Lips, 2019). This also means that thermal contrasts during CUs tend to increase over time.

Another impact to consider is the influence of low water temperatures due to CU on local cooling of air temperature above land. The heat exchange between the sea and land is partially maintained by the cross-shore breeze (Figure 9). The landward penetration of the daily sea breeze usually reaches 10—50 km in temperate zones while nightly land breeze may reach ca 10 km seaward (Miller et al., 2003).

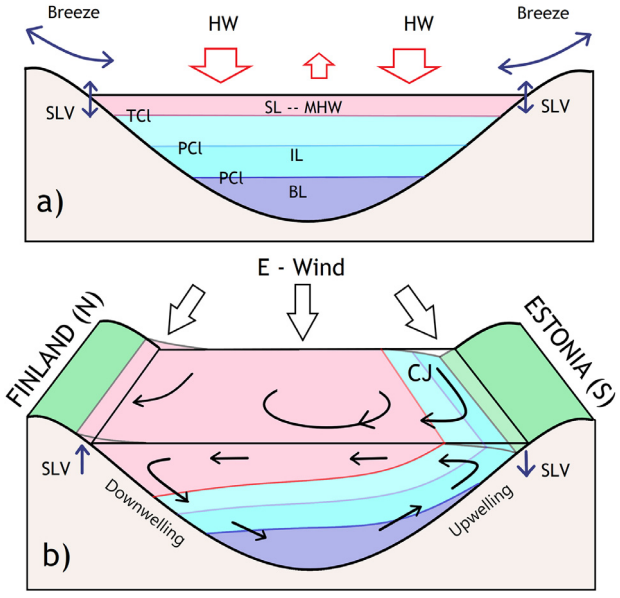

Figure 9 Scheme of HW — heat wave events (a) and wind-driven upwelling-downwelling pairing in the Gulf of Finland (b). (a): HW causes MHW (marine heat wave events) in the surface layer (SL), while the heat transfers into intermediate (IL) and bottom layers (BL) with gradually increasing salinity are restricted by thermocline (TCl) and pycnoclines (PCl). Coastal breeze mediates heat transfers between sea and land, also causing diurnal sea level variations (SLV) at the coast. (b): At the Estonian coast, easterly wind causes alongshore coastal jet (CJ), rise of pycnoclines, upwelling, and local SL lowering. Westerly would basically turn the scheme around (upwelling along Finnish coast and downwelling at Estonian coast); controlled by topography, Coriolis force and friction, the current patterns may be more complex basin-wise. Differing from the steady state (a), the simultaneous occurrence of HW and CU (or CUs slowly switching between opposing coasts) enable more effective heat transfer to the water mass (b).

Statistically, Kunda is slightly warmer than the 45 km inland Väike-Maarja station (5.7 vs. 4.9°C according to the EWS statistics). This is because Väike-Maarja is located 120 m higher than Kunda and considering environmental lapse rate, one can expect ca 0.8°C lower temperatures there. According to the comparison of air temperature differences between Kunda and Väike-Maarja stations, the cooling effect during the CU events compared to the rest of the studied period (Figure 10) was 0.9°C in terms of average temperatures and 1.5°C in daily maxima. More specifically, during the studied HW, Kunda was 1.2°C warmer than Väike-Maarja, while during HW and CU combined, the Kunda location was only 0.3°C warmer. In some CU days, instead of being 1°C warmer, the maxima at Kunda were up to 5 degrees lower than in Väike-Maarja (Figure 10). Such influence of cool nearshore currents is also known on a grander scale. For instance, cold Benguela current-affected Namib coast is climatologically ca. 3—5 degrees cooler than areas less than 100 km inland (Lancaster et al., 1984). The influence is similar in the case of the cold Humboldt current near the Chilean coast, however, without a very clear thermal pattern due to mountainous inland terrain.

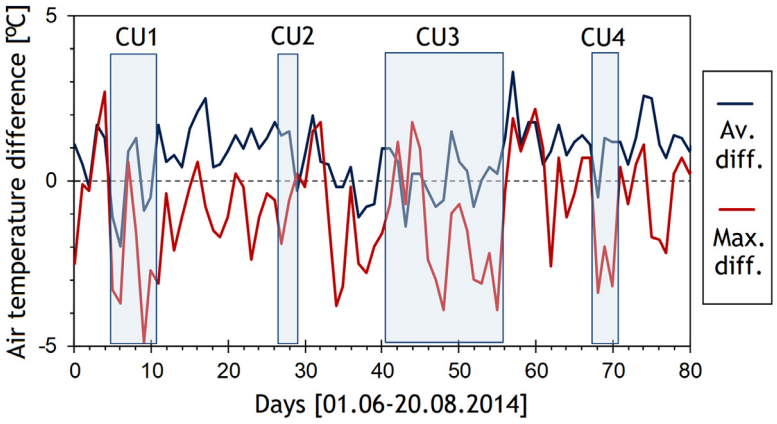

Figure 10 Temporal variations in air temperature differences between Kunda (coastal) and Väike-Maarja (inland) stations, showing cooling effect (i.e. larger negative differences) of CU events on Kunda's daily average (Av.) and maximum (Max.) air temperatures.

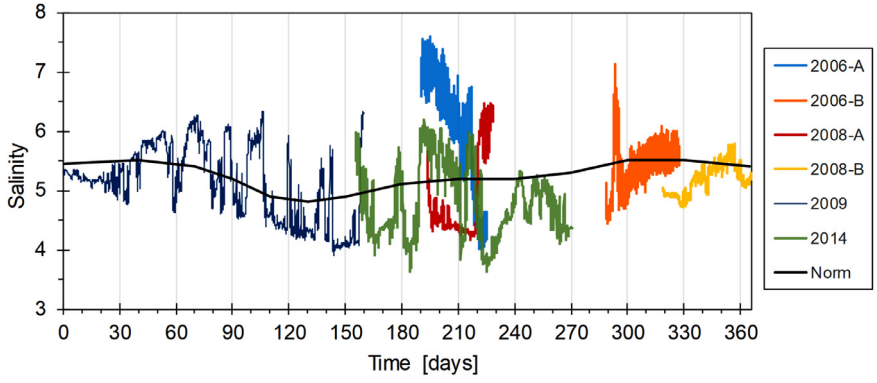

Figure 11 Salinity variations at Letipea according to RDCP measurements performed in different moorings (see also Suursaar, 2010; 2013) plotted against days in year. Always corresponding to CU events, the abrupt changes for 1–3 units mask the feeble seasonality in statistical norm (e.g. Alenius et al., 1998). Slightly higher maxima in 2006 partly occur as a result of slightly deeper mooring in that year (ca 11.5 m vs. ca 10.5 m).

Finally, the possible ecological effects of HW and CU on biota increasingly deserve attention. Generally, adverse effects of MHWs on biota are relatively well-known (Meier et al., 2019; Oliver et al., 2019; Panch et al., 2013). It is reasonable to assume that under global warming, HWs and MHWs are becoming more frequent and intense in different environments worldwide – at least relative to local climatic normals, but also in absolute terms. On a local scale, CUs may occasionally mitigate such overheating effects by cooling down the water mass (Figures 3, 9). However, CUs also serves as a nutrient pump, lifting up nutrient-rich water from the deep to surface, promoting thus productivity and triggering algal blooms (e.g. Jiang and Wang, 2018; Kononen and Nõmmann, 1992). Moreover, although introducing some variability, CUs cannot stop the overall basin-wide warming trends. Continuation of water temperature rise and intensification of MHWs in combination with CUs, causing abrupt changes in water temperature (e.g. Figure 3), salinity (e.g. Figure 11) and other interrelated parameters, put ecosystems under additional stress by challenging the established tolerance limits of species or entire communities (Paalme et al., 2020; Takolander et al., 2017; Wernberg et al., 2013).

4. Conclusions

(1) Summer 2014 HW (also called 2014 Swedish heat wave) manifested in the Gulf of Finland area by extraordinary high air and water temperatures. Air temperatures reached 32°C on 31 July and the daily normals were exceeded by 5°C at Kunda weather station (North Estonia) in several episodes lasting for 3, 5, and 7 consecutive days. At Narva-Jõesuu station, water temperatures stayed between 20 and 26.5°C during 44 consecutive days in July and August while at Kunda coastal station the MHWs were frequently interrupted by upwellings. Both HW and CU effects were captured by the RDCP measurements at Letipea Peninsula, lasting for 115 days from 6 June to 29 September 2014.

(2) Caused by a stable anticyclonic weather pattern and persisting E-winds, CUs evolved along the southern coast of the Gulf in four episodes (3–7.06, 26–29.06, 10–17.07, 5–7.08). Occurring on the background of a MHW, the maximum water temperature dropped by up to 17°C within a few days. At the 10 m deep RDCP mooring location, an 18.6°C drop (from 21.5 to 2.9°C) occurred within 60 hours on 3–5 August. In addition to up to

20°C variations in water temperatures, the CUs were also accompanied by salinity fluctuations between 3.6 and 6.2, and relatively fast West-directed alongshore current (coastal jet). The CU-related West current was especially favoured in upper layers and it was the statistically preferred current mood, which frequently flowed against the wind.

(3) In terms of local climate, the cooling effect of the CUs occasionally mitigated the overheating effects by HWs both in the sea and above the land (via breezes operating at the marine-land boundary). However, CUs cannot stop the overall basin-wide warming trends. In elongated channel-like basins like the Gulf of Finland, being major mixing agents, upwelling at one coast is usually paired with downwelling at the opposite coast. The simultaneous or subsequent occurrence of HWs and CUs effectively contributes to heat transfer from the atmosphere to the deeper water mass. Because heating of the water mass in the process of global warming begins from the sea surface and lags behind in the deeper layers, also thermal contrasts during CUs may increase in the future. Hence, rising extremes of HWs and rapid variations by CUs may increasingly put ecosystems under stress and trigger undesirable changes.

Acknowledgements

The study was financially supported by the Estonian Research Council grant PUT1439 and marine environment monitoring project LLOMI14064. We thank the EWS for the Estonian weather data and the Finnish Environment Institute (SYKE) for the SST images.

References

Alenius, P., Myrberg, K., Nekrasov, A., 1998. The physical oceanography of the Gulf of Finland: a review. Boreal Environ. Res. 3, 97—125.

Andrejev, O., Myrberg, K., Alenius, P., Lundberg, P., 2004. Mean circulation and water exchange in the Gulf of Finland — a study based on three-dimensional modelling. Boreal Environ. Res. 9 (1), 1—16.

Cheng, L., Abraham, J., Zhu, J., Trenberth, K.E., Fasullo, J., Boyer, T., Locarnini, R., Zhang, B., Yu, F., Wan, L., Chen, X., Song, X., Liu, Y., Mann, M.E., 2020. Record-setting ocean warmth continued in 2019. Adv. Atmos. Sci. 37 (2), 137—142. https://doi.org/10.1007/s00376-020-9283-7.

Cole, S., Jacobs, P., 2020. NASA, NOAA Analyses Reveal 2019 Second Warmest Year on Record. NASA Press Release 20-003, https://www.nasa.gov/press-release/nasa-noaa-analyses-reveal-2019-second-warmest-year-on-record, (accessed 22 May 2020).

Delpeche-Ellmann, N., Mingelaitė, T., Soomere, T., 2017. Examining Lagrangian surface transport during a coastal upwelling in the Gulf of Finland. Baltic Sea. J. Mar. Syst. 171, 21—30, https://doi.org/10.1016/j.jmarsys.2016.10.007.

Delpeche-Ellmann, N., Soomere, T., Kudryavtseva, N., 2018. The role of nearshore slope on cross-shore surface transport during a coastal upwelling event in Gulf of Finland. Baltic Sea. Estuar. Coast. Shelf Sci. 209, 123—135, https://doi.org/10.1016/j.ecss.2018.03.018.

Easterling, D.R., Meehl, G.A., Parmesan, C., Changnon, S.A., Karl, T.R., Mearns, L.O., 2000. Climate extremes: observations, modeling, and impacts. Science 289, 2068—2074.

Elken, J., Lehmann, A., Myrberg, K.The BACC II Author Team, 2015. Recent Change — Marine Circulation and Stratification. In: Second Assessment of Climate Change for the Baltic Sea Basin. Springer, Cham, 131—144, https://doi.org/10.1007/978-3-319-16006-1_7.

Frich, P., Alexander, L.V., Della-Marta, P., Gleason, B., Haylock, M., Klein Tank, A., Peterson, T., 2002. Global changes in climatic extremes during the 2nd half of the 20th century. Clim. Res. 19, 193—212, https://doi.org/10.3354/cr019193.

Gidhagen, L., 1987. Coastal upwelling in the Baltic Sea — satellite and in situ measurements of sea-surface temperatures indicating coastal upwelling. Estuar. Coast. Shelf Sci. 24 (4), 449—462.

Gill, A.E., Clarke, A.J., 1974. Wind-induced upwelling, coastal currents and sea-level changes. Deep-Sea Res. 21, 325—345.

Haapala, J., 1994. Upwelling and its influence on nutrient concentration in the coastal area of the Hanko Peninsula, entrance of the Gulf of Finland. Estuar. Coast. Shelf Sci. 38 (5), 507—521.

Hobday, A.J., Oliver, E.C.J., Sen Gupta, A., Benthhuysen, J.A., Burrow, M.T., Donat, M.G., Holbrook, N.J., Moore, P.J., Thomsen, M.S., Wernberg, T., Smale, D.A., 2018. Categorizing and naming marine heatwaves. Oceanography 31 (2) 162—173, https://doi.org/10.5670/oceanog.2018.205.

Hoegh-Guldberg, O., Bruno, J.F., 2010. The impact of climate change on the World's marine ecosystems. Science 328, 1523—1528.

EWS, 2020. Estonian Weather Service; http://www.ilmateenistus.ee/kliima/weather-events/?lang=en, (accessed 22 May 2020).

IPCC 2014. IPCC Fifth Assesment Report (AR5), https://www.ipcc.ch/report/ar5/.

Jiang, R., Wang, Y.-S., 2018. Modeling the ecosystem response to summer coastal upwelling in the northern South China Sea. Oceanologia 60 (1) 32—51, https://doi.org/10.1016/j.oceano.2017.05.004.

Kallis, A., Loodla, K., Tillmann, E., Krabbi, M., Pärg, R., Vint, K., Jõeveer, A., Juust, E., 2015. Yearbook of Estonian Meteorology 2014. Tallinn, 162 pp., (in Estonian), http://www.ilmateenistus.ee/wp-content/uploads/2016/02/aastaraamat_2014.pdf (Accessed on 22 May 2020).

Keevallik, S., Soomere, T., Pärg, R., Žukova, V., 2007. Outlook for wind measurement at Estonian automatic weather stations. Proc. Estonian Acad. Sci.-Eng. 13 (3), 234—251.

Keevallik, S., Vint, K., 2015. Temperature extremes and detection of heat and cold waves at three sites in Estonia. Proc. Estonian Acad. Sci. 64 473—479, https://doi.org/10.3176/proc.2015.4.02.

Kononen, K., Nõmmann, S., 1992. Spatio-temporal dynamics of the cyanobacterial blooms in the Gulf of Finland, Baltic Sea. In: Carpenter, E.J., Capone, D.G., Rueter, J.G., et al. (Eds.). In: Marine pelagic cyanobacteria: Trichodesmium and other Diazotrophs. NATO ASI Ser., vol. 362. Springer, Dordrecht, 95—113.

Kont, A., Jaagus, J., Orviku, K., Palginõmm, V., Ratas, U., Rivis, R., Suursaar, Ü., Tõnisson, H., 2011. Natural development and human activities on Saaremaa Island (Estonia) in the context of climate change and integrated coastal zone management. In: Schernewski, G., Hofstede, J., Neumann, T. (Eds.), Global change and Baltic coastal zones. Springer, Dordrecht 117—134, https://doi.org/10.1007/978-94-007-0400-8_8.

Kotta, J., Herkül, K., Jaagus, J., Kaasik, A., Raudsepp, U., Alari, V., et al., 2018. Linking atmospheric, terrestrial and aquatic environments in high latitude: Regime shifts in the Estonian regional climate system for the past 50 years. PLOS ONE 13 (12), art. no. e0209568, https://doi.org/10.1371/journal.pone.0209568.

Kowalewski, M., Ostrowski, M., 2005. Coastal up- and downwelling in the southern Baltic. Oceanologia 47 (4), 453—475.

Kowalewska-Kalkowska, H., Kowalewski, M., 2019. Combining

Satellite Imagery and Numerical Modelling to Study the Occurrence of Warm Upwellings in the Southern Baltic Sea in Winter. Remote Sens. 11 (24), art. no. 2982, https://doi.org/10.3390/rs11242982.

Lancaster, J., Lancaster, N., Seely, M.K., 1984. Climate of the central Namib Desert. Madoqua 14 (1), 5—61.

Lehmann, A., Myrberg, K., Höflich, K., 2012. A statistical approach to coastal upwelling in the Baltic Sea based on the analysis of satellite data for 1990—2009. Oceanologia 54 (3), 369—393, https://doi.org/10.5697/oc.54-3.369.

Lenssen, N.J.L., Schmidt, G.A., Hansen, J.E., Menne, M.J., Persin, A., Ruedy, R., Zyss, D., 2019. Improvements in the GISTEMP uncertainty model. J. Geophys. Res. Atmos. 124, 6307—6326, https://doi.org/10.1029/2018JD029522.

Liblik, T., Lips, U., 2019. Stratification has strengthened in the Baltic Sea — an analysis of 35 years of observational data. Front. Earth Sci. 7, art. no. 174, https://doi.org/10.3389/feart.2019.00174.

Lips, I., Lips, U., Liblik, T., 2009. Consequences of coastal upwelling events on physical and chemical patterns in the central Gulf of Finland (Baltic Sea). Cont. Shelf Res. 29, 1836—1847, https://doi.org/10.1016/j.csr.2009.06.010.

Meier, H.E.M., Dieterich, C., Eilola, K., Gröger, M., Höglund, A., Radtke, H., Saraiva, S., Wåhlström, I., 2019. Future projections of record-breaking sea surface temperature and cyanobacteria bloom events in the Baltic Sea. Ambio 48, 1362—1376, https://doi.org/10.1007/s13280-019-01235-5.

Miller, S.T.K., Keim, B.D., Talbot, R.W., Mao, H., 2003. Sea breeze: Structure, forecasting, and impacts. Rev. Geophys. 41 (3), 1—31, https://doi.org/10.1029/2003RG000124.

Myrberg, K., Andrejev, O., 2003. Main upwelling regions in the Baltic Sea — a statistical analysis based on three-dimentional modelling. Boreal Environ. Res. 8, 97—112.

Oliver, E.C.J., Burrows, M.T., Donat, M.G., Sen Gupta, A., Alexander, L.V., Perkins-Kirkpatrick, S.E., Benthuysen, J.A., Hobday, A.J., Holbrook, N.J., Moore, P.J., Thomsen, M.S., Wernberg, T., Smale, D.A., 2019. Projected Marine Heatwaves in the 21st Century and the Potential for Ecological Impact. Front. Mar. Sci. 6, art. no. 734, https://doi.org/10.3389/fmars.2019.00734.

Õispuu, T.-M., 2019. Heat waves in Estonia in 1951—2018. In: Järvet, A. (Ed.). Yearbook of Estonian Geographical Society, Vol. 44 Tallinn, 93—110, (in Estonian, English summary), http://egs.ee/wp-content/uploads/2019/12/EGS_Aastaraamat_44kd.pdf, (Accessed May 22, 2020).

Paalme, T., Torn, K., Martin, G., Kotta, I., Suursaar, Ü, 2020. Littoral benthic communities under effect of heat wave and upwelling events in NE Baltic Sea. J. Coast. Res., Spec. Issue 95, 133—137. https://doi.org/10.2112/SI95-026.1.

Panch, C., Scotti, M., Barboza, F.R., Al-Jaabi, B., Brakel, J., Briski, E., Bucholz, B., Franz, M., Ito, M., Paiva, F., Saha, M., Sawall, Y., Weinberger, F., Wahl, M., 2013. Heat waves and their significance for temperate benthic community: A near-natural experimental approach. Glob. Chang. Biol. 24, 4357—4367, https://doi.org/10.1111/gcb.14282.

Perkins, S.E., Alexander, L.V., 2013. On the measurement of heat waves. J. Clim. 26, 4500—4517, https://doi.org/10.1175/JCLI-D-12-00383.1.

Rafferty, J.P., 2020. Heat wave. Britannica online: https://www.britannica.com/science/heat-wave-meteorology, (accessed 22 May 2020).

Russo, S., Dosio, A., Graversen, R.G., Sillmann, J., Carrao, H., Dunbar, M.B., Singleton, A., Montagna, P., Barbola, P., Vogt, J.V., 2014. Magnitude of extreme heat waves in present climate and their projection in a warming world. J. Geophys. Res. Atmos. 119 (22), 12,500—12,512, https://doi.org/10.1002/2014JD022098.

Russo, S., Sillmann, J., Fischer, E.M., 2015. Top ten heatwaves since 1950 and their occurrence in the coming decades. Environ. Res. Lett. 10, art. no. 124003, https://doi.org/10.1088/1748-9326/10/12/124003.

Rutgersson, A., Jaagus, J., Schenk, F., Stendel, M., Bärring, L., Briede, A., Claremar, B., Hanssen-Bauer, I., Holopainen, J., Moberg, A., Nordli, Ø., Rimkus, E., Wibig, J.The BACC II Author Team, 2015. Recent Change — Atmosphere. In: Second Assessment of Climate Change for the Baltic Sea Basin. Springer, Cham, 69—97, https://doi.org/10.1007/978-3-319-16006-1_4.

Schlitzer, R., 2020. Ocean Data View, https://odv.awi.de.

Schär, C., Vidale, P.L., Lüthi, D., Frei, C., Häberli, C., Liniger, M.A., Appenzeller, C., 2004. The role of increasing temperature variability in European summer heatwaves. Nature 427, 332—336.

Shaltout, M., 2019. Recent sea surface temperature trends and future scenarios for the Red Sea. Oceanologia 61 (4), 484—504, https://doi.org/10.1016/j.oceano.2019.05.002.

Siegel, H., Gerth, M., 2019. Sea Surface Temperature in the Baltic Sea in 2018. HELCOM Baltic Sea Environment Fact Sheets 2019 https://helcom.fi/baltic-sea-trends/environment-fact-sheets/hydrography/sea-surface-temperature-in-the-baltic-sea-in-2018/, (accessed May 22, 2020).

Smid, M., Russo, S., Costa, A.C., Granell, C., Pebesma, E., 2019. Ranking European capitals by exposure to heat waves and cold waves. Urban Clim. 27, 388—402, https://doi.org/10.1016/j.uclim.2018.12.010.

Soomere, T., Myrberg, K., Leppäranta, M., Nekrasov, A., 2008. The progress in knowledge of physical oceanography of the Gulf of Finland: a review for 1997—2007. Oceanologia 50 (3), 287—362.

Strange, E., Fernando, H., 2001. Entrainment and mixing in stratified shear flows. J. Fluid Mech. 428, 349—386.

Suursaar, Ü., Aps, R., 2007. Spatio-temporal variations in hydro—physical and -chemical parameters during a major upwelling event off the southern coast of the Gulf of Finland in summer 2006. Oceanologia 49 (2), 209—228.

Suursaar, Ü., 2010. Waves, currents and sea level variations along the Letipea—Sillamäe coastal section of the southern Gulf of Finland. Oceanologia 52 (3), 391—416, https://doi.org/10.5697/oc.52-3.391.

Suursaar, Ü., 2013. Locally calibrated wave hindcasts in the Estonian coastal sea in 1966—2011. Est. J. Earth Sci. 62 (1), 42—56, https://doi.org/10.3176/earth.2013.05.

Takolander, A., Cabeza, M., Leskinen, E., 2017. Climate change can cause complex responses in Baltic macroalgae: A systematic review. J. Sea Res. 123, 16—26, https://doi.org/10.1016/j.seares.2017.03.007.

Talpsepp, L., 2008. On the influence of the sequence of coastal upwellings and downwellings on the surface water salinity in the Gulf of Finland. Estonian J. Eng. 14 (1), 29—41.

Uiboupin, R., Laanemets, J., 2009. Upwelling characteristics derived from satellite sea surface temperature data in the Gulf of Finland, Baltic Sea. Boreal Environ. Res. 14 (2), 297—304.

Westerlund, A., Tuomi, L., Alenius, P., Miettunen, E., Vankevich, R.E., 2018. Attributing mean circulation patterns to physical phenomena in the Gulf of Finland. Oceanologia 60 (1), 16—31, https://doi.org/10.1016/j.oceano.2017.05.003.

Westerlund, A., Tuomi, L., Alenius, P., Myrberg, K., Miettunen, E., Vankevich, R.E., Hordoir, R., 2019. Circulation patterns in the Gulf of Finland from daily to seasonal timescales. Tellus A 71, art. no. 1627149, https://doi.org/10.1080/16000870.2019.1627149.

Wernberg, T., Smale, D.A., Tuya, F., Thomsen, M.S., de Langlois, T.J., Bettignies, T., Bennett, S., Rousseaux, C.S., 2013. An extreme climatic event alters marine ecosystem structure in a global biodiversity hotspot. Nat. Clim. Chang. 3, 78—82, https://doi.org/10.1098/rspb.2012.2829.